



Article

# Effect of Sequential Thermal Aging and Water Immersion on Moisture Kinetics and SBS Strength of Wet Layup Carbon/Epoxy Composites

Vistasp M. Karbhari <sup>1,\*</sup>  and SoonKook Hong <sup>2</sup>

<sup>1</sup> Department of Civil Engineering, Department of Mechanical & Aerospace Engineering, University of Texas Arlington, Arlington, TX 76019, USA

<sup>2</sup> Department of Mechanical and Naval Architectural Engineering, Naval Academy, Changwon City 440-746, Kyungsangnam-do, Korea

\* Correspondence: vkarbhari@uta.edu

**Abstract:** This paper presents results of specific cases of sequential exposure of wet layup ambient cured carbon/epoxy composites to thermal aging and immersion in deionized water. Thermal aging is conducted at temperatures between 66 °C and 260 °C for periods of time up to 72 h whereas immersion is up to 72 weeks. Effects are characterized in terms of moisture kinetics using a two-stage diffusion model, and through short beam shear (SBS) strength. The response is characterized by a competition between the mechanisms of postcure, which results in increased polymerization and increases in SBS strength and glass transition temperature; and thermally induced microcracking and polymer degradation as well as moisture-induced plasticization and hydrolysis accompanied by fiber-matrix debonding, which results in deterioration. Thermal aging by itself is not seen to negatively impact SBS strength until the highest temperatures of exposure are considered in the investigation. However, the subsequent immersion in deionized water is seen to have a greater deteriorative effect with the period of post-thermal aging immersion being the dominant deteriorative factor.

**Keywords:** thermal aging; water; short beam shear (SBS); deterioration; postcure; carbon/epoxy composite



**Citation:** Karbhari, V.M.; Hong, S. Effect of Sequential Thermal Aging and Water Immersion on Moisture Kinetics and SBS Strength of Wet Layup Carbon/Epoxy Composites. *J. Compos. Sci.* **2022**, *6*, 306. <https://doi.org/10.3390/jcs6100306>

Academic Editor: Vijay Kumar Thakur

Received: 6 September 2022

Accepted: 8 October 2022

Published: 11 October 2022

**Publisher's Note:** MDPI stays neutral with regard to jurisdictional claims in published maps and institutional affiliations.



**Copyright:** © 2022 by the authors. Licensee MDPI, Basel, Switzerland. This article is an open access article distributed under the terms and conditions of the Creative Commons Attribution (CC BY) license (<https://creativecommons.org/licenses/by/4.0/>).

## 1. Introduction

Because of their tailorability, high specific performance attributes, light weight, ease of fabrication and placement in the field, corrosion resistance, and relatively high comparative durability, fiber-reinforced polymer (FRP) composites are used in a range of structural applications in the aerospace, marine/naval, automotive, and civil infrastructure areas. Historically, carbon fibers have often been preferred in high-performance applications such as in the aerospace sector due to the high axial stiffness attributes, relatively higher strength characteristics, lack of susceptibility to moisture uptake and deterioration at the fiber level, resistance to creep and stress-rupture under sustained loading, and significantly better fatigue resistance when used in the form of unidirectional composites. Based on cost considerations, their use in offshore, marine/naval, and civil structural applications is predicated on the use of non-autoclave cure, wet layup, and infusion-based processes. These, generically, have a lower level of initial polymerization and slower cure progression, fiber content, and greater variability in properties [1] than prepreg-based autoclave cured aerospace composites. Due to this, the extensive set of data and specifications from the aerospace sector are not directly applicable. Historically, the use of these non-aerospace composites has been accompanied by excessively conservative, and high, factors of safety [2,3] leading to the use of composites being not as cost-effective as otherwise possible. There is, thus, a continuing need for focused studies related to the durability of ambient- and moderate-temperature cure, non-automated process-based composites [4–7] under a wide range of

environmental conditions including solution and heat exposure over extended periods of time to develop a more comprehensive understanding of deterioration over time and better factors of safety.

While carbon fibers are inert to most environmental exposure conditions likely to be faced in such applications, they do oxidize at elevated temperatures exceeding 500 °C [8–11]. Some studies have shown oxidative degradation in air in the 430–760 °C range. While fibers having higher nitrogen content have been reported to degrade at lower levels [12], research on carbon-fiber-based rocket nozzles indicates negligible decomposition until about 700 °C [13]. The integrity and performance of the composite, however, depends intrinsically on the matrix and the fiber-matrix interface, both of which are affected by moisture and temperature. The effects of moisture uptake include degradation of the polymer itself through interruption of hydrogen bonds by water molecules [14–16], decreases in strength characteristics [16], swelling [17], and increased interfacial deterioration [1,4,18,19]. Nogueira et al. [16] showed that moisture uptake decreased with an increase in the degree of cure due to the higher crosslink density of the resulting polymer network which caused a decrease in the presence of molecule-sized holes in the network structure, leading to lower levels of free volume. Glass transition temperature ( $T_g$ ) is known to decrease with an increase in moisture content [20–22]. This is, however, complicated by the effect of curing [23] and the progression of cure due to immersion in aqueous solutions [24,25]. Cure progression, and hence increases in levels of  $T_g$  of ambient temperature cured composites, have been noted to be accelerated under conditions of immersion in water at elevated temperatures [26,27]. The effects of moisture uptake, both under ambient conditions and as a result of immersion at elevated temperatures, on mechanical properties of carbon-fiber-reinforced composites fabricated using ambient temperature cure and non-automated processes for infrastructure and naval/marine applications have been extensively reported on [27–31], including as related to the effect of marine environments and exposure to seawater and simulated seawater solutions [4,32–35].

Exposure to elevated temperature regimes can be of concern for these materials since polymer matrix composites are susceptible to thermooxidative degradation at temperatures between 100–350 °C, with the effects being accelerated as the glass transition temperature is reached and exceeded. The effects can include those of reversible thermal aging which results in decreased molecular mobility and an increased evolution of strain and damage. In addition, as temperature levels and time of exposure are increased, irreversible volumetric-based chemical aging occurs which includes chain scission reactions and additional crosslinking, both of which can result in changes to the surface diffusion response. Thermal aging in air can lead to superficial oxidation which results in cracking without application of the load [36–38]. This furthers the diffusion of oxygen into the material resulting in additional deeper oxidation reactions and damage [39]. The yield strength of the resin and the interface bond between the resin and the fiber decrease with an increase in temperature [40], with shear stiffness and interfacial shear strength decreasing as a function of temperature in epoxy-based composites [40,41]. Wimolkatisak and Bell [42] noted that the stiffness of the resin was initially reduced by exposure to an elevated temperature, giving fibers freedom to move which could result in further degradation of even fiber-dominated characteristics. Given the importance of these phenomena on the stability and durability of polymer composites in the civil, marine, and naval areas, there has been extensive study of composites exposed to fire [8,43–49]. While a significant body of work exists for autoclave-cured, aerospace-grade carbon fiber composites, significantly less is known about these materials as fabricated through wet layup and non-autoclave-cured processes [50], especially as related to the competing effects of initial cure progression and the deteriorative effects at temperatures lower than  $T_g$  and/or where the effects are due to radiant heat rather than actual contact with the flame.

Beyond the effects of temperature through direct contact with flames, it is critical to understand materials-level processes and characterize the residual performance attributes of composites after thermal exposure in cases where the composites are routinely, or on

occasion, as in the case of industrial processes or gas flares, exposed to elevated temperature regimes for extended periods of time between a few hours to a few days [47,51]. It should be noted that such events also occur when flammable liquids with vapor pressure at levels greater than atmospheric are released from pressurized storage [52] and in cases of deflagration events from waste transport and storage [53]. In the offshore area, composites are increasingly used on oil rigs and platforms and may face events of high temperature radiant heat requiring assurances of post-incident structural integrity [54]. In the offshore environment, fires, though rare, can continue for extended periods of time [46,55–58], exposing structural elements located outside the direct influence of the fire—but close enough for radiant heat exposure—to high temperature levels for extended periods of time. In addition, fires adjacent to FRP cladding can also result in such exposure conditions [46]. In marine/naval and offshore applications, the structure and FRP materials used therein are exposed to conditions of immersion and moisture exposure, and are expected to continue to perform as designed after such events.

Thermal aging can affect not just residual properties but also subsequent moisture uptake, which in turn would further affect performance characteristics. The effect of thermal spikes and prior thermal conditioning of aerospace prepreg-based, autoclave-processed composites on moisture uptake has been shown to result in a larger reduction in  $T_g$  and greater uptake levels [59–62]. However, relatively little is known about the moisture kinetics of ambient cured carbon/epoxy materials after extended periods of heat exposure that may exceed the glass transition temperature. Lu et al. [63] reported on the effects of prior thermal aging on subsequent water uptake behavior of pultruded BFRP plates in one of the only reports on non-autoclave composites, reporting that prior thermal exposure resulted in both the postcure and deterioration of the fiber-matrix bond, resulting in increased diffusion coefficients and lowered activation energies. Hamidi et al., based on research conducted on non-autoclave-cured composites, emphasized that very little was known about the effects of prior thermal history on moisture absorption dynamics of such materials that have a greater susceptibility to environmental exposure faced during service [64].

The current investigation focuses on the assessment of moisture kinetics and effects on short beam shear (SBS) strength performance as a result of immersion in water after thermal exposure for periods of up to 72 h at temperatures between ambient and 260 °C, representative of the cases described earlier of extended periods of high heat/thermal energy. To assess residual performance characteristics, short beam shear tests are conducted following specific periods of immersion, up to 72 weeks, in deionized water. This study is expected to provide insight into post-event stability and operational feasibility of structural components formed from wet layup ambient cure-based carbon/epoxy composites and is part of a larger study aimed at the characterization of the long-term response of these materials.

## 2. Materials and Methods

### 2.1. Material System

The carbon-fiber-reinforced polymer composite consisted of a unidirectional carbon fabric of an aerial weight of 644 g/m<sup>2</sup>, with carbon fibers having a nominal tensile strength, modulus, and density of 3.79 GPa, 230 GPa, and 1.74 g/cm<sup>3</sup>, respectively. The resin was a difunctional Bisphenol A/epichlorohydrin-derived liquid epoxy (Epon-828-based) with an epoxide equivalent weight of 185–192 g/cc and a number average molecular weight of about 700. A polyetheramine-modified polyoxypropylenediamine curing agent with an average molecular weight of about 400 was used to derive a resin system with a viscosity of 600–700 cps at 25 °C, and a pot-life of 3–4 h with a cured density of 1.15 g/cm<sup>3</sup>. Both the fibers and resin were representative of systems already being used in the field in applications similar to those addressed by the current investigation. Epoxy resins are preferred here due to their higher toughness and better long-term performance characteristics under conditions of ambient temperature cure and subsequent thermal loading.

Composite specimens were fabricated with two layers of the carbon fabric using the wet layup process using only manual roller-based pressure without the use of vacuum bags to simulate field conditions. Panels were cured under controlled conditions of 23 °C and 30% relative humidity for seven days after which they were postcured for 72 h at 60 °C to enable a uniform level of cure progression. The fiber mass fraction was determined using acid digestion procedures to be 60% (i.e., a fiber volume fraction of 49.8%) with a standard deviation of 2–2.5% over all specimens.

## 2.2. Specimens, Exposure Conditions, and Test Methods

### 2.2.1. Specimens

The current investigation focuses on two aspects of post-exposure, response-moisture uptake and kinetics and short beam shear (SBS) strength characteristics. The former was assessed using specimens of nominal size of 25.4 mm × 25.4 mm cut from plates. Five specimens were used for each measurement. Mechanical characteristics were assessed using short beam shear specimens of 6 mm × 18 mm size cut from the same plates. The choice of SBS specimens was based on the expected deteriorative effects of thermal aging and the subsequent immersion in solution on the interfaces between layers of reinforcing fabric and at the fiber-matrix interface. The short beam shear test has been shown previously to be a powerful tool for the assessment of effects of moisture-associated durability of composites [65,66] since interlaminar shear strength is often the limiting factor for composites because the through thickness characteristics, and overall integrity, are matrix dependent.

### 2.2.2. Exposure Conditions

After cutting specimens to size and inspecting them for surface defects and edge voids (the presence of which resulted in rejection of specimens), the specimens were stored in a humidity chamber at 23 °C and 30% RH for two weeks prior to further exposure. Specimens were then subjected to a set of exposure conditions as detailed in this section and shown schematically in Figure 1. A set of SBS specimens were tested under ambient conditions as a baseline. Additional specimens were thermally aged at temperatures between 150 °F and 500 °F at intervals of 50 °F, i.e., at 66 °C, 93 °C, 121 °C, 149 °C, 177 °C, 204 °C, 232 °C, and 260 °C for periods of time ranging from 1 to 72 h. In each case, the specimens were placed in a furnace that was already at temperature, then maintained at the specified temperature for the assigned period of time, removed, and then allowed to cool back to 23 °C before further action. Specimens for moisture uptake were then placed in deionized water baths maintained at 23 ± 1 °C for periods up to 72 weeks. SBS specimens were carefully inspected for outliers that showed excessive deterioration in terms of delamination due to local defects and were divided into three batches. The first set was tested for residual properties. The second set consisted of specimens thermally aged for 8 h over the range of temperatures, and the third set consisted of specimens exposed to a temperature of 232 °C over a range of exposure periods. The latter two sets and a set of unexposed specimens (i.e., not subject to any thermal aging) were placed in the water baths for further exposure through immersion in deionized water. The non-thermally aged specimens provided a baseline for comparison of the individual and combined exposures (thermal aging followed by immersion in deionized water).

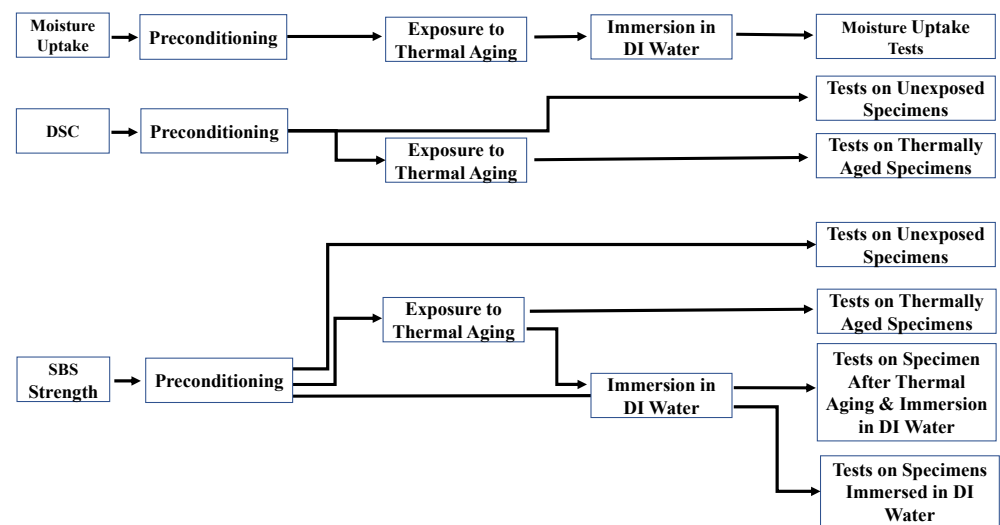


**Figure 1.** Schematic of exposure conditions.

### 2.2.3. Test Methods

Short beam shear tests were conducted following ASTM D 2344 [67] at a crosshead speed of 1 mm/min with the load being applied until failure. In the case of thermally aged specimens, testing was conducted after cooling back to 23 °C under ambient conditions to obtain residual properties. Data analysis for outliers was conducted by inspection and in accordance with MIL-HDBK-1F procedures [68]. In the case of specimens immersed in deionized water, specimens were removed periodically using padded tweezers to ensure minimal pressure and no transfer of oil or substances from human hands that could inadvertently contaminate the specimens and or the deionized water bath, patted dry with tissue paper, and then weighed to measure uptake after which they were reinserted into the baths. The time period for the operation was standardized for consistency and to avoid effects of varying levels of evaporation through the specimens.

To characterize the effects of thermal aging on the cure and glass transition temperature of the specimens, tests were also conducted using differential scanning calorimetry (DSC) following ASTM D3418 [69]. Specimens of 10–15 mg mass were heated at a rate of 10 °C/min from 0 to the final temperature of 160 °C in a controlled nitrogen environment at a flow rate of 10 mL/min.

## 3. Results and Discussion

Results of the investigation are reported in this section initially as related to moisture uptake and kinetics and then as related to the short beam shear tests. Tests related to moisture uptake were conducted on specimens after thermal aging between 23 °C and 260 °C for periods of time ranging between 1 and 72 h, followed by immersion in deionized water for periods up to 72 weeks. SBS tests were conducted on specimens exposed to four sets of conditions: (a) prior to thermal aging, (b) after thermal aging between 23 °C and 260 °C for periods of time ranging between 1 and 72 h, (c) after thermal aging for eight hours over the range of temperatures followed by immersion in deionized water for periods up to 72 weeks, and (d) after thermal aging at 232 °C for periods of time between 1 and 72 h followed by immersion in deionized water for periods up to 72 weeks. The first two sets provide the unexposed and residual properties after extended periods of thermal exposure whereas the other two sets provide insight into continued performance in aqueous environments after exposure to heat.

### 3.1. Moisture Uptake and Kinetics

While the Fickian model [70,71] is commonly used to describe diffusion in composites, it does not, as such, address aspects of chemical interaction between the solution molecules

and the polymer network, nor the relaxation and deterioration that is often seen as moisture ingress progresses. Two-stage models have been shown to better represent this, especially as related to systems having both an initial concentration gradient-driven diffusion process and a time-dependent process based on relaxation and deterioration that lead to a slower approach to an equilibrium uptake level [72,73]. In wet layup composites, the situation is further complicated by competing effects of cure progression (which in the case of ambient cure can be accelerated by water uptake) and the deteriorative effects of irreversible matrix microcracking and fiber-matrix debonding. The present study uses the two-stage model proposed by Bao et al. [73] wherein uptake is described by

$$\frac{M_t}{M_{eq}} = (1 + k\sqrt{t}) \left\{ 1 - \exp \left[ -7.3 \left( \frac{Dt}{h^2} \right)^{0.75} \right] \right\} \quad (1)$$

where  $M_t$  is the moisture uptake at any time  $t$ ,  $M_{eq}$  and  $D$  are the equilibrium moisture uptake level (also termed the transition level since it represents the transition between the two stages) and diffusion coefficient associated with stage one uptake, respectively,  $h$  is the specimen thickness, and  $k$  is the time-dependent coefficient characteristic of the rate of polymer relaxation and damage due to water absorbed. When  $k = 0$ , equation 1 reverts to the Fickian form of diffusion modeled by Shen and Springer [71]. It is noted that in the current study, specimens aged at the highest temperature of exposure, 260 °C, showed significant surface deterioration and severe debonding between fibers and resin for aging periods exceeding 8 h, resulting in large drops in SBS strength. The level of surface damage and the creation of additional paths for wicking of water due to fiber-matrix debonding results in excessive, and rapid, water uptake with subsequent loosening of resin particles. This level of deterioration makes the study of water uptake and the resulting residual strength impractical and hence, tests were only conducted on specimens aged between 1 and 8 h at 260 °C.

Moisture uptake is seen to follow a two-stage process. The first stage is concentration gradient controlled and predominantly Fickian, showing initial rapid diffusion. The second slower, and significantly longer, stage is associated with relaxation and deteriorative processes. In the second stage, there is both a rearrangement of polymer chains as the water molecules penetrate [73] and the filling of the new free volume created by the reactions with these molecules, resulting in a slower process as depicted by the lower slope. As seen from the representative moisture uptake traces, an ultimate equilibrium concentration is not approached, even asymptotically, over the 72-week period, indicating that the time scale for the second stage is much longer than that of diffusion, with extremely long relaxation regimes of the resin and interface regions in the glassy phase. As seen in Figure 2 for all temperatures of exposure, the diffusion parameter,  $D$ , increases with time of prior thermal aging until the 16 h level for all temperatures up to 204 °C. This increase is in line with the effect of postcure which results in an increase in free volume as crosslink density increases [23,74–76]. It should be noted that an analogy can be drawn with earlier results that reported the dependence of the diffusivity coefficient on the hydrothermal aging temperature [71]. In that case, an increase in the temperature of the solution in which the specimens were aged caused acceleration in the Brownian motion of the water molecules, resulting in an increase in the rate of diffusion. In the current case, the previous history of elevated temperature exposure affects the potential for pathways of ingress and reactivity within the resulting polymer network, and in the composite. While it is not clear if the results of prior temperature exposure followed by immersion in a solution are similar to those of simultaneous immersion in higher temperature solutions, there is a level of similarity to the phenomenon of increases in diffusion in moisture uptake through thermal spikes [59–62]. It should be noted that in the current case, there are multiple competing phenomena at play, including postcure, resulting from the exposure to elevated temperature, the effect of thermal exposure itself on the free volume and structure the polymer network, and deterioration of interfacial bonds due to microcracking between

fabric layers within resin-rich areas and in the fiber matrix interfacial regions at the highest level of exposure where the greatest deterioration is likely to take place. As seen in Figure 2, specimens thermally aged for 1–8 h at 260 °C show an exponential increase in the diffusion coefficient due to wicking into the microcracks and gaps between the fiber and matrix, with the value of the diffusion coefficient for specimens exposed to 8 h at 260 °C being three times that of the unexposed (i.e., no thermal aging) specimens.

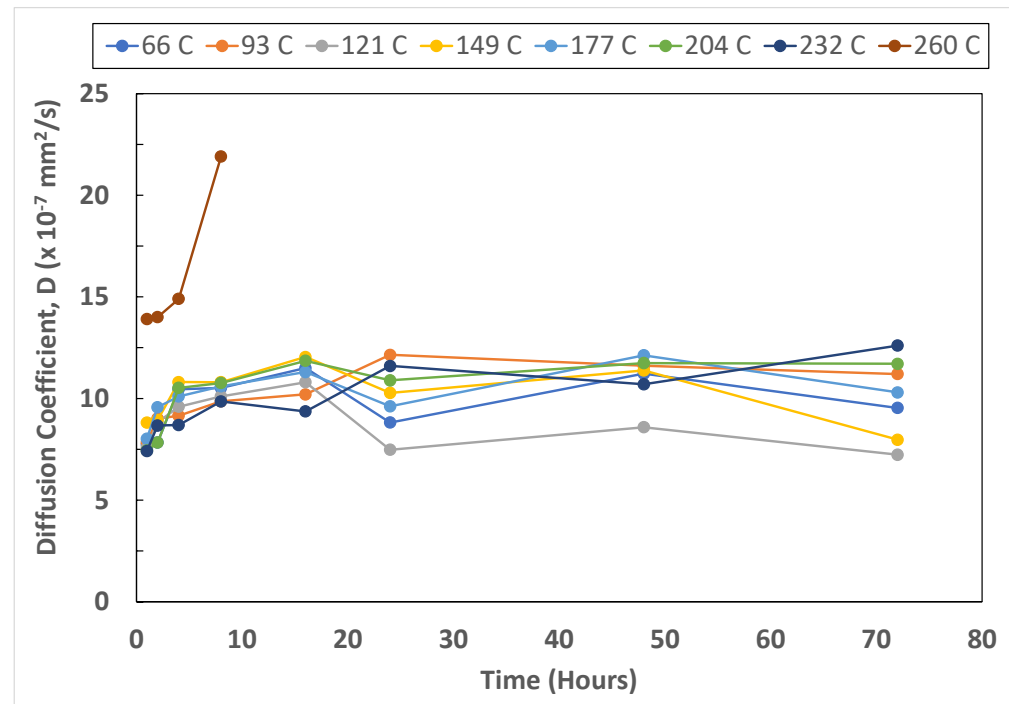


**Figure 2.** Diffusion coefficients as a function of time and temperature of prior thermal aging.

It is of interest to note that for all temperature levels except 93 °C and 232 °C, the diffusion coefficient decreases after the 16 h level, with diffusion coefficients remaining lower than the peak level. This is indicative of the decrease in reactivity of epoxy groups once crosslinking has peaked. For specimens thermally aged at 93 °C, the levels of the coefficient of diffusion are the highest at 24 h and then decrease but remain above the 16 h peak level. In the case of 232 °C, the diffusion coefficient continues to increase, which is indicative of the deterioration in the bulk resin and the fiber matrix interface which results in greater wicking along these microstructural defect areas in an auto-accelerative manner noted earlier by Marom [77] and Woo and Piggott [78] and is similar to the behavior seen from specimens exposed to the highest temperature level of 232 °C. These levels of dramatic increase due to damage would indicate substantive decreases in interfacial shear strength, which is confirmed, as will be described later, though SBS testing. It should be emphasized that values of  $D$  for all levels of thermal aging and exposure are higher than those of the non-thermally aged specimens.

While fairly clear trends are noted for the relationship between the coefficient of diffusion,  $D$ , as a function of previous temperature of thermal aging and time of exposure, the same is not true of the coefficient representative of relaxation/deterioration,  $k$ . This is due to the more complex interactions that characterize the processes taking place over the longer time scale that are related to plasticization, and to structural reordering and redistribution of the free volume elements [79], which is further complicated by the lock-in effects of extended periods of elevated temperature exposure followed by immersion in deionized water. Overall results, normalized by the value of the time-dependent relaxation coefficients for specimens immersed in deionized water but not subjected to thermal aging,  $k = 1.76 \times 10^{-3} \text{ mm}^2/\text{s}$ , are shown in Figure 3. It is noted that while there is significant

variation in values at lower time periods of thermal aging, the range narrows with an increase in time of exposure, as would be expected of relaxation-type phenomena. The highest levels of coefficients are seen after 1 and 2 h of thermal aging at 177 °C, which corresponds to the region where the glass transition temperature,  $T_g$ , as measured by DSC, of specimens after thermal aging was the highest. Specimens aged at the highest temperature of exposure, 260 °C, as expected, show an increase in the value of  $k$ , which is representative of relaxation/deterioration mechanisms, with a rapid increase up to 4 h after which any further increase was very small.

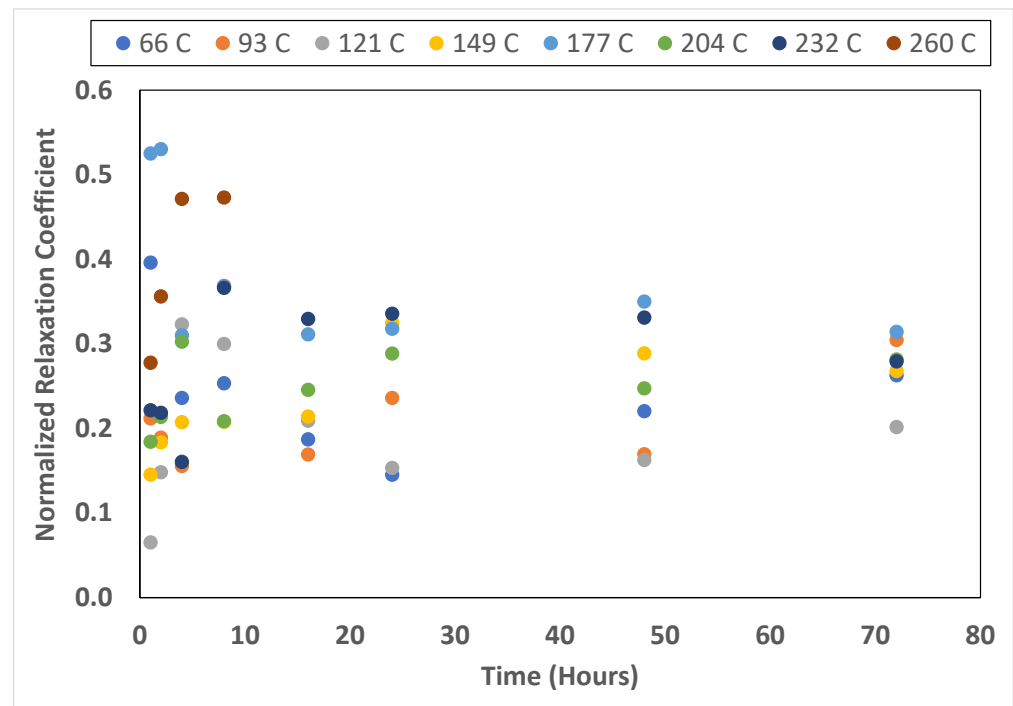
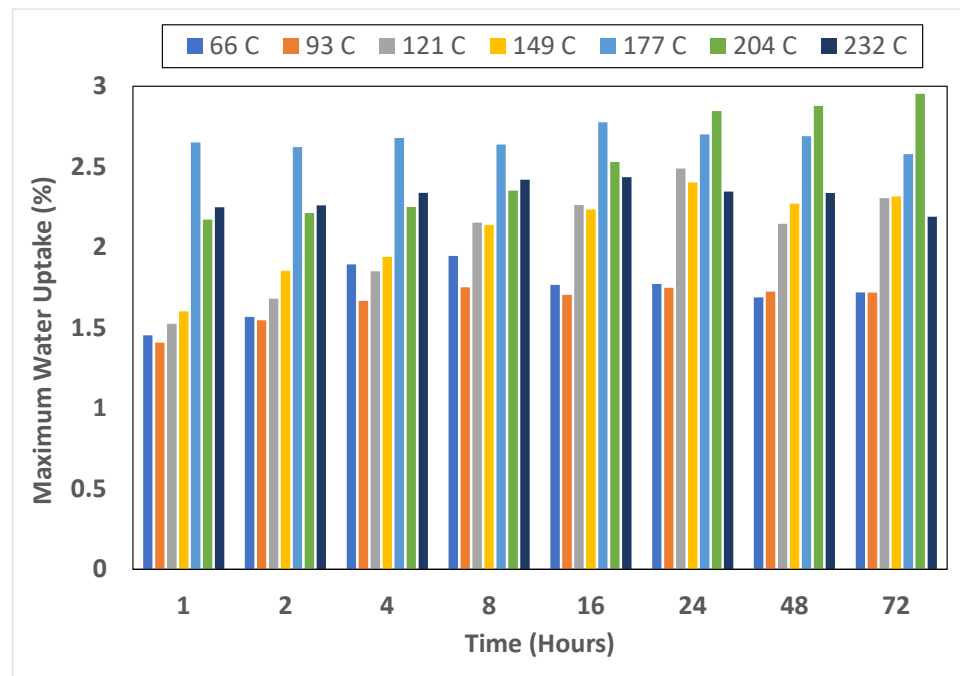


**Figure 3.** Normalized relaxation coefficient as a function of time and temperature of prior thermal aging.

The two-stage diffusion response is characterized by a transition from the relative rapid diffusion-based regime to the slower relaxation/deterioration-dominated regime [27,63,73]. The moisture uptake level associated with stage one uptake is significantly lower than the maximum moisture uptake level,  $M_{max}$ , recorded at the end of the period of immersion of 72 weeks. It is thus of interest to further study key points of moisture uptake as related to the prior effects of the level of thermal aging as seen in Figure 4a–c. As seen in Figure 4a, the level of moisture uptake, representative of the peak uptake rather than just the uptake at the end of the period of immersion, shows a general trend of increasing with the temperature of thermal aging for the same period of time for temperatures up to 177 °C for times up to 16 h, and for temperatures up to 204 °C for times between 24 and 72 h. These trends are in line with the expected increase in uptake with prior thermal aging. The drop at the two highest levels can be associated with decreased free volume due to changes in polymer network structure at these levels. It is noted that the experimental values for the peak moisture uptake varied within sets by less than 2.5%.

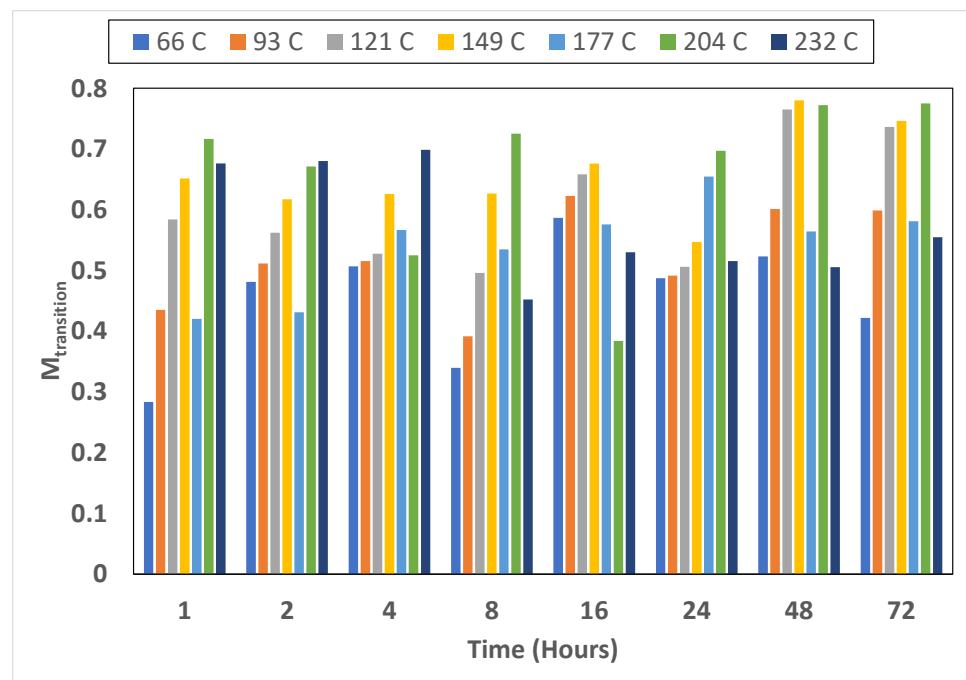
In comparison, the level of transition, representative of the point of change in uptake from a diffusion-dominated first stage to the slower second stage of uptake due to polymer relaxation and damage, increases with the temperature of aging for the same period of time for all times of thermal aging until 149 °C, as shown in Figure 4b. After this temperature, there is variation based on time of exposure due to the changes in network structure and overall damage in the composite. The initial trends are in accordance with earlier results related to moisture absorption and temperature related to the degree of cure attainment

reported by Tang and Springer [80]. This is also in accord with results by Chatterjee and Gillespie [81] that the first stage of the moisture uptake ends later as the degree of polymerization increases since the extended periods of temperature exposure result in increasing polymerization of the wet layup ambient cured composites considered in the current investigation. It is noted that as the degree of polymerization increases, the free volume increases [74,75], but simultaneously, water molecules need greater energy to diffuse across the network and fill the free volume [82]. When seen in light of the ratio of uptake prior to the transition to the peak uptake level, as in Figure 4c, it is of interest to note trends of an initial increase followed by a decrease, indicating that the effects of relaxation/deterioration on moisture uptake increase as a function of temperature to a greater extent than due to the time of aging. This has important ramifications for post-event assessment as related to structural effectiveness. It is also noted that at the longest period of exposure of 72 h, the ratio for the three highest temperatures of aging fall within a very narrow band of between 22.5% and 26.2%, indicating a similarity of overall response.

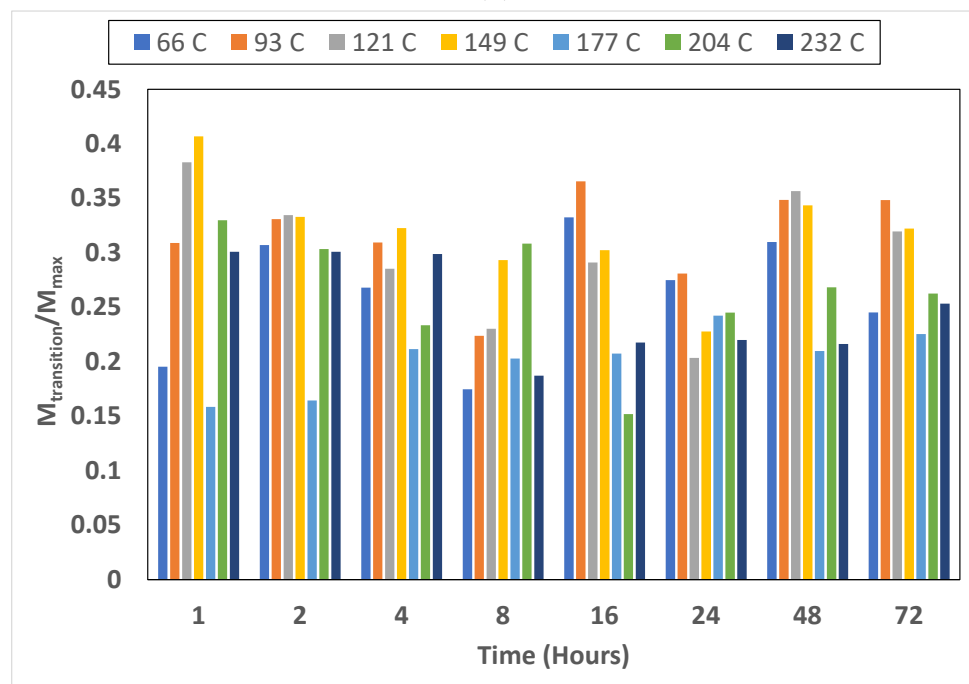


(a)

Figure 4. Cont.



(b)



(c)

**Figure 4.** (a): Level of maximum water uptake as a function of time and temperature of prior thermal aging. (b): Level of water uptake at the transition point as a function of time and temperature of prior thermal aging. (c): Ratio of water uptake at the transition point to the maximum uptake as a function of time and temperature of prior thermal aging.

### 3.2. Short Beam Shear Strength after Thermal Aging

In this section, the effects of thermal aging on residual SBS strength are discussed first, followed by the effects of post-aging immersion in deionized water. While most previous studies on the effects of temperature prior to immersion in solution have been due to thermal shock regimes [59–62], the case considered herein is of extended, rather

than extremely short, periods of thermal aging followed by immersion, which is more representative of the combinations likely to be seen in naval/marine and civil infrastructure elements.

Thermal aging at all temperatures except the two highest levels resulted in SBS strength values higher than those at the initial unexposed level as shown in Figure 5. This indicates that postcure processes have a greater positive effect than that of deterioration due to aging except at temperatures of 232 °C and 260 °C. It is of interest to note that while the unexposed specimens show an increase of 7.6% in SBS strength over the 72 h period under consideration, thermal aging resulted in an increase of 21% at 93 °C and 177 °C and 23.4% at 149 °C. When viewed in terms of the overlap due to scatter, these are essentially similar. At 66 °C, the maximum increase in residual strength is the lowest at 17.7% and at 260 °C, it is the highest at 27.1%. The maximum degradation in SBS strength is noted at the highest temperature of thermal aging of 260 °C with the decrease occurring within three different regimes of 4–8 h (at a rate of 11.4% per hour), 8–24 h (at a rate of 4% per hour), and from 24–72 h where the decrease was the slowest at a rate of 1% per hour. As seen in Figure 5, all temperatures of thermal aging result in an increase in residual SBS strength followed by a decrease over longer periods of exposure in line with results reported earlier by Zavatta et al. [83]. As mentioned earlier, the increases are due to postcure through exposure to elevated temperatures which results in an increase in the degree of cure as reported by Vora et al. [84]. It is thus of interest to assess the level of increase in SBS strength, and the time taken to achieve the peak as a function of temperature of aging keeping in mind the competition between mechanisms of cure progression and thermal deterioration. Figure 6 shows the comparison indicating that as temperature increases, the time taken to attain peak SBS strength decreases, with the maximum being reached after 4 h of exposure at 260 °C. At 232 °C, the same time period of aging results in a peak that is 4% lower. Peaks attained after 8 h for temperatures between 121 °C and 204 °C result in the SBS strength increasing only from 47.93 MPa to 48.08 MPa, well within scatter bounds, over with this range. The initial mode of failure is one of interlaminar fracture, as would be expected of SBS specimens, with a transition to one dominated by fiber-matrix debonding and interlayer separation with increasing levels of thermal aging, as was also noted by Akay et al. [85]. The transition can be seen through a comparison of SEM images of failure for unexposed specimens (Figure 7a), where there is good bonding between the fiber and matrix; to one where debonding has been initiated but hackles are still seen in the matrix with a bond between the fiber and matrix, as noted for specimens after 48 h of thermal aging at 177 °C (Figure 7b); to one where there is extensive debonding with fiber surfaces in the pullout zones not having a significant matrix or adhering to them (Figure 7c). The latter is representative of results of thermal aging at 232 °C for 48 h and above, and at 260 °C at 8 h and above.

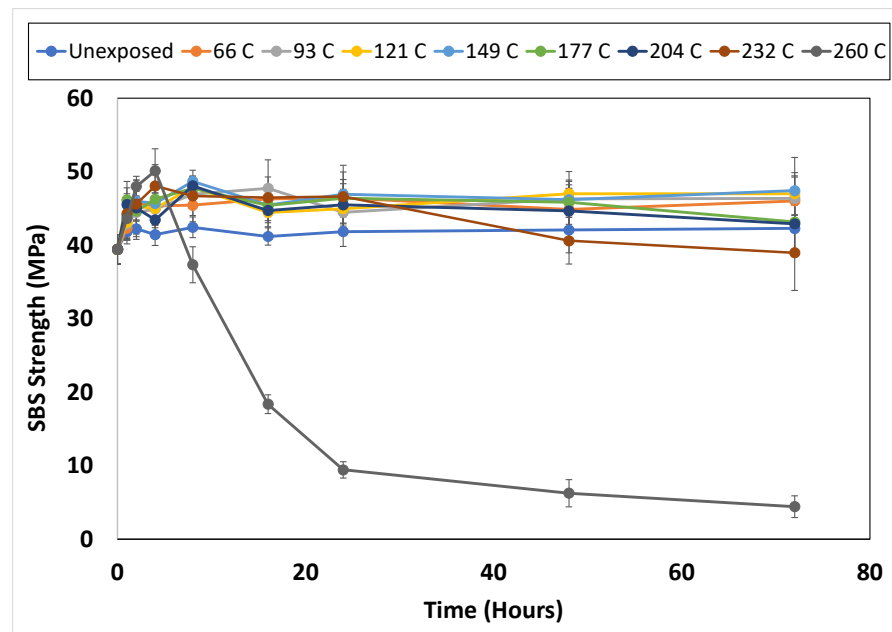


Figure 5. Residual SBS strength as a function of time and temperature of thermal aging.

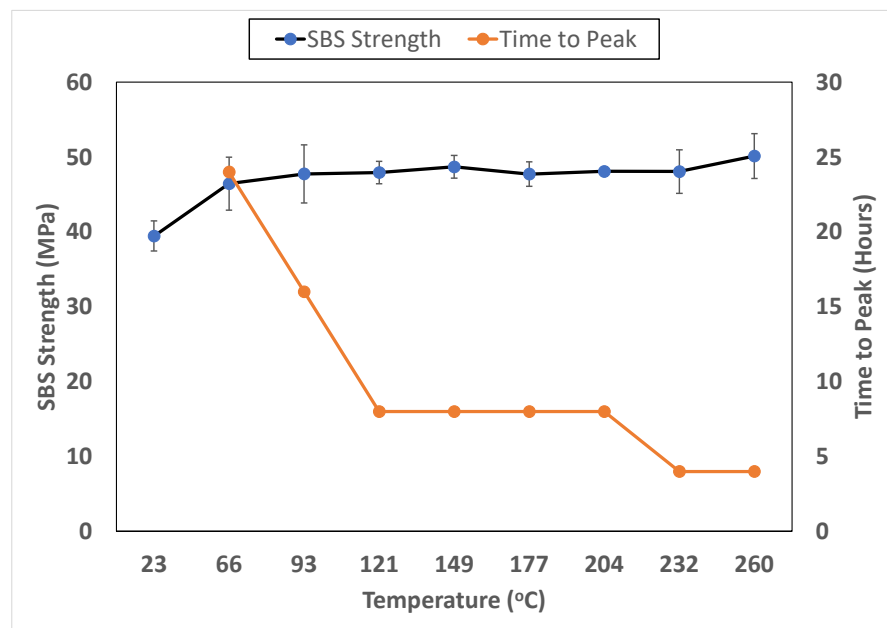
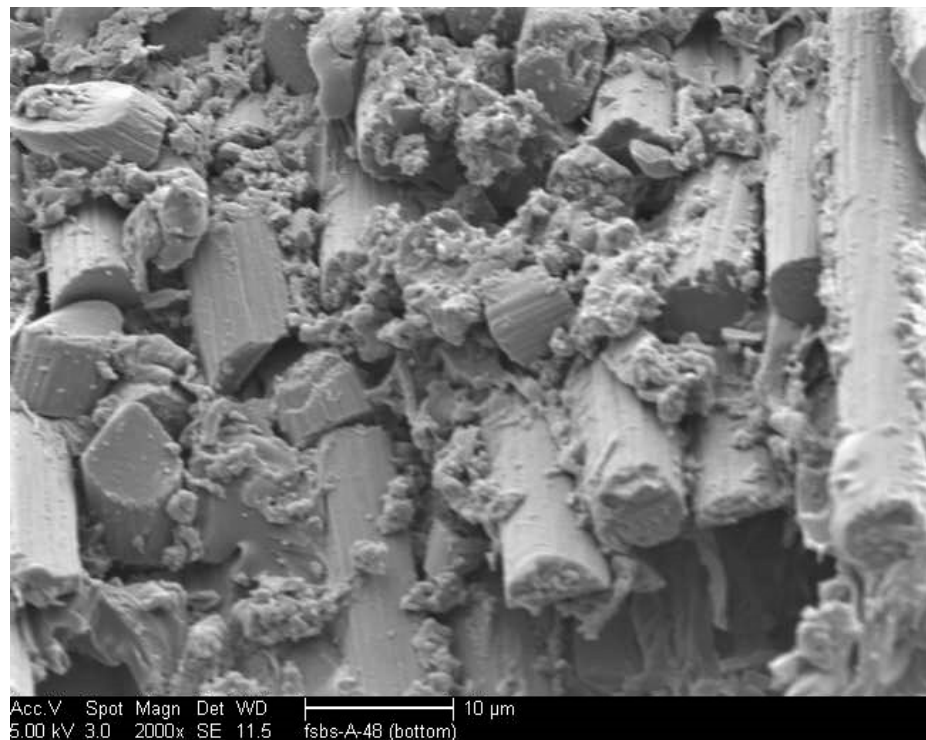
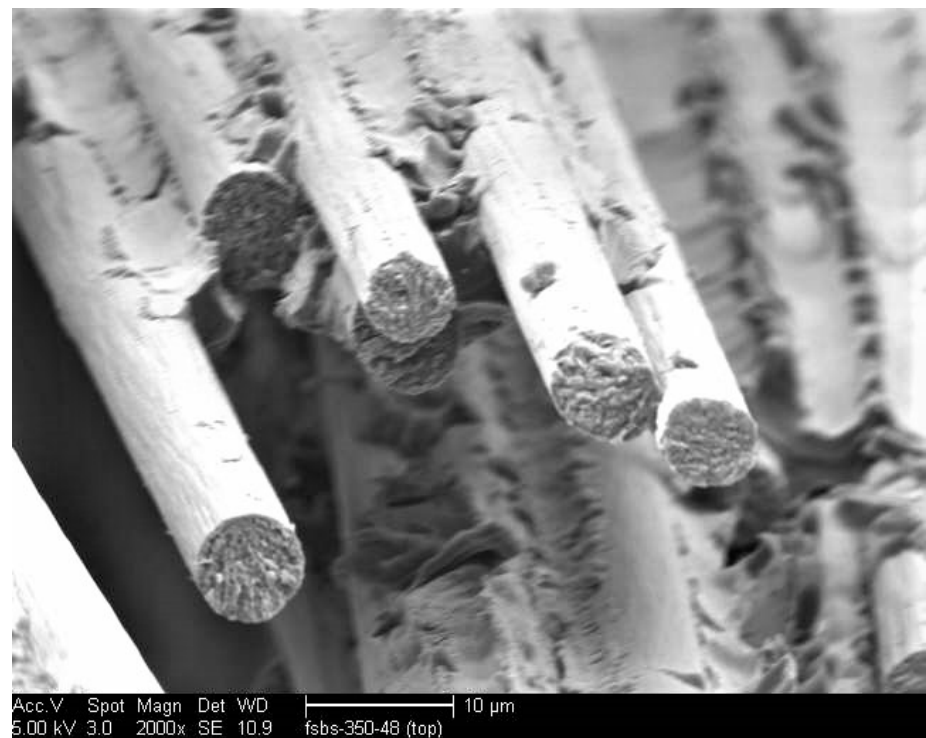


Figure 6. Comparison of peak SBS strength and time to attain the peak as a function of temperature of thermal aging.

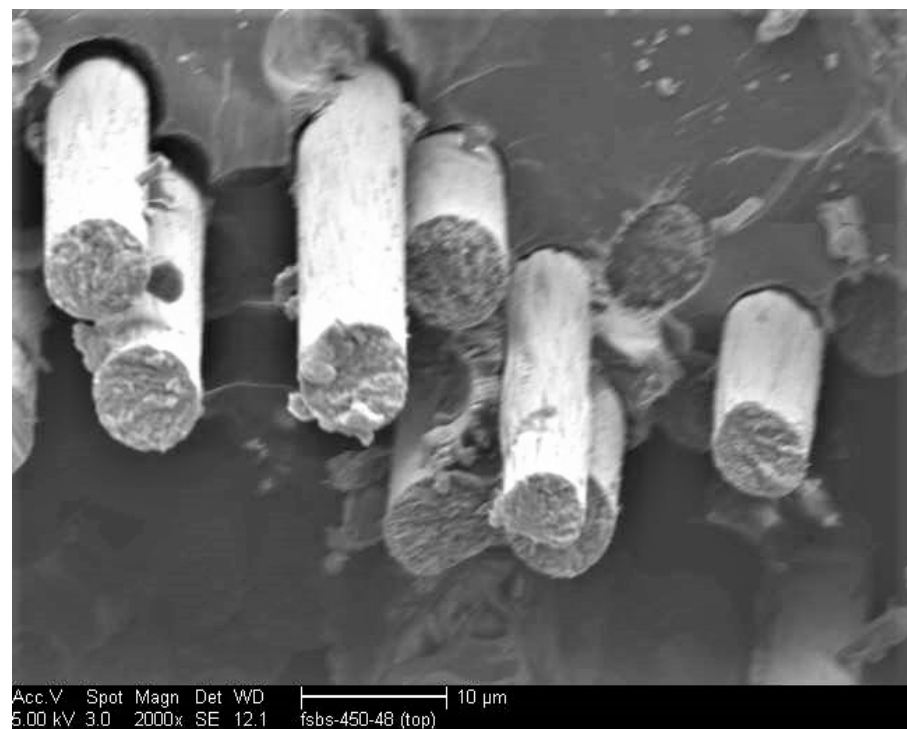


(a)



(b)

Figure 7. Cont.



(c)

**Figure 7.** (a) SEM image of fracture of an unaged specimen. (b): SEM image showing debonding along with hackles on the matrix for a specimen subject to 48 h of thermal aging at 177 °C. (c): SEM image showing debonded areas with gaps between the fiber and matrix and clean fiber surfaces.

As noted earlier, thermal aging results in a competition between an increase in SBS strength as a consequence of increased polymerization due to the exposure to elevated temperature, and a decrease due to deterioration as a consequence of microcracking due to mismatch between the thermal expansion coefficients of the carbon fiber and the epoxy resin as well as surface cracking, crazing, and deterioration due to extended periods of exposure to elevated temperatures. It is thus of interest to assess, at least on a comparative basis, the actual level of overall change as measured by the difference between the level that might have been attained through the progression of postcure without the effects of deterioration, and the performance level measured through testing after each period of thermal aging (as shown in Figure 5). As a first approximation, this can be estimated through the identification of the peak level of overall SBS strength, of 50.13 MPa after 4 h of thermal aging at 260 °C, and assuming it to be the maximum level of performance increase attainable due to postcure alone; and then using a power law fit at each temperature of aging for SBS strength until the peak to assess deterioration. The use of a power law has its basis in the description of creep [86], which is relevant here due to the effects of postcure and relaxation within the competing phenomena. Results of this can be seen for each temperature of aging in Figure 8, from which it can be noted that the difference between the thermal aging curves and the postcure curves is a comparative assessment of deterioration due to thermal aging, which is obscured when the results of just Figure 5 are assessed since the effects of the competing phenomena are not separated. This shows that at the longest period of aging, 72 h, deterioration is noted even at the lowest temperatures of aging and is 7.8%. In comparison, levels at 93 °C, 121 °C, 149 °C, 177 °C, 204 °C, 232 °C, and 260 °C are 7.5%, 6.2%, 5.4%, 13.9%, 14.4%, 22.3%, and 91.2%, respectively. The initial decrease in levels between 66 °C and 149 °C emphasizes the increasing positive effect of postcure and strength over that of deterioration as a consequence of thermal aging, while the increase after that point indicates a transition to increasing dominance of thermal-aging-based

deteriorative mechanisms. This subtle difference from the conclusions that might otherwise be drawn solely based on Figure 5 is critical.

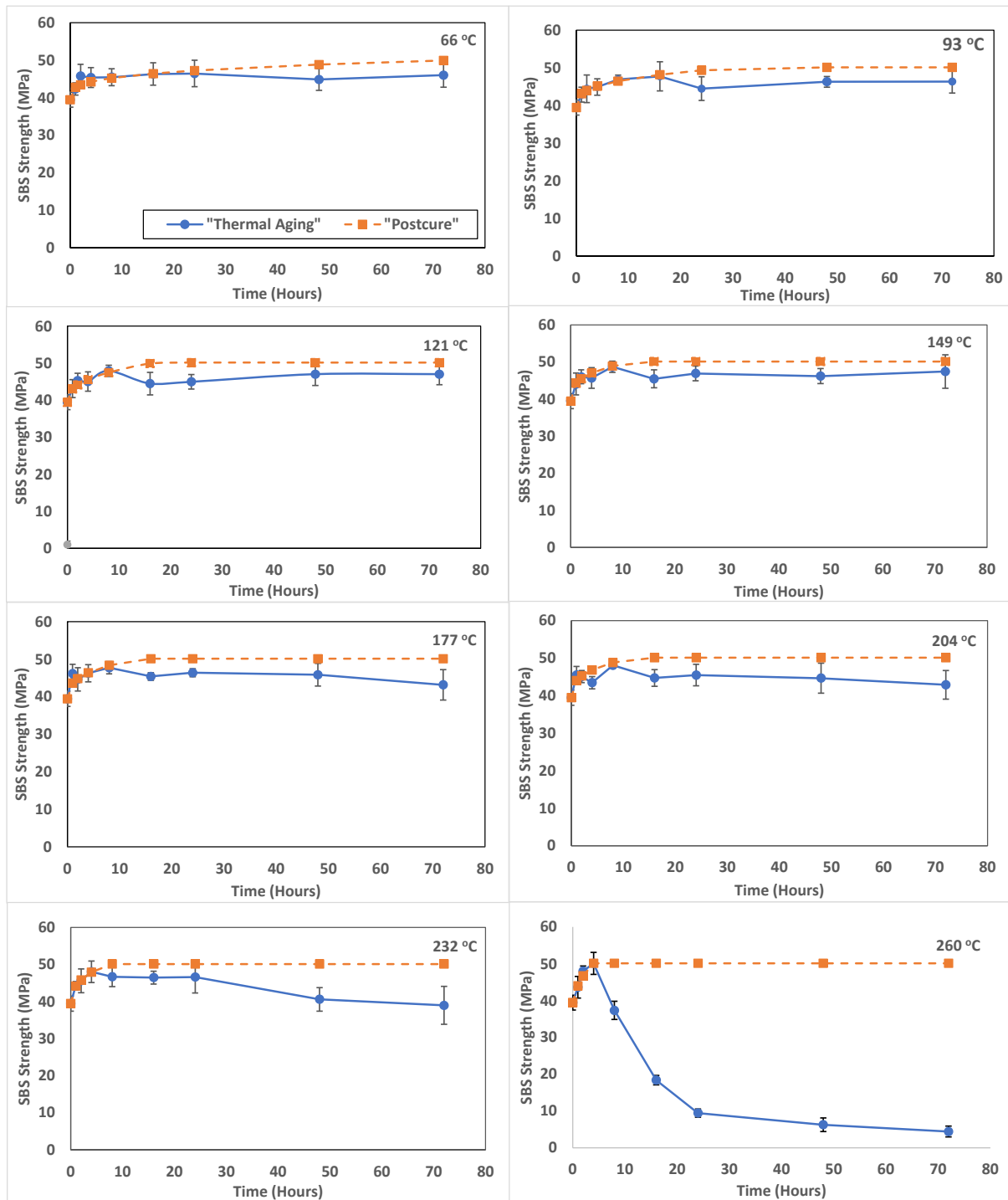


**Figure 8.** Comparison of effects of thermal aging with predicted postcure levels as a function of time and temperature of aging.

### 3.3. Effects of Aqueous Immersion after Thermal Aging

As discussed earlier, there are a number of cases where structures and components subjected to thermal aging are subsequently exposed to moisture/solution. To assess the effects of this combination of exposures, two specific sets of thermal aging conditions prior to aqueous immersion were considered: (a) 8 h of thermal aging over the range of

temperatures considered in this study, and (b) a range of exposure periods at 232 °C. The two cases were specifically chosen to highlight effects of sequential thermal and aqueous exposures under key transitional conditions that would help explain overall trends from a more limited set of tests. The 8 h level of thermal aging represents both a transition in relaxation as noted from the moisture kinetics data through the relaxation coefficient and a transition in mechanical response after thermal aging as seen in Figures 5 and 6. The second case, at the 232 °C level, is representative of the highest temperature, at which changes even over the longest period of aging did not result in SBS strength decreasing below the initial unexposed control. Decreases of 18.9% and 22.3% are, however, noted from the peak SBS strength and assumed postcure levels of SBS strength, respectively.

The effect of immersion in deionized water on specimens thermally aged for 8 h over the range of temperatures on SBS strength is shown in Figure 9, from which it can be seen that immersion results in a decrease for all specimens, with the general trend being an initial rapid decrease followed by a largely asymptotic region between 12 weeks and 48 weeks followed by a second period of rapid decrease. For purposes of clarity in seeing data, standard deviations are not shown in Figure 9 but are listed in Table 1, from which it can be seen that for all sets except the two highest levels of thermal aging, the range of standard deviations is less than 10%. Specimens that were previously thermally aged at 232 °C show this range until the 48-week level when the standard deviation was 13.9% and at the 72-week level when it increased to 18%. For specimens aged at 260 °C, however, standard deviations with the exception of the 16 h level are all above 10%, with the maximum being for specimens at the end of the immersion period of 72 weeks at 31.6%. It should be noted that as described earlier, thermal aging at this temperature resulted in excessive surface and internal cracking, resulting in non-uniform and excessive water uptake for specimens beyond 8 h of thermal aging, which results in even further damage in local areas resulting in the excessive variation in results. Nonetheless, it is clear that the maximum deterioration is seen in the specimens thermally aged at 260 °C for 8 h, with the level of decrease from the initial level (i.e., prior to immersion in deionized water) being 49.3%. In comparison, the level for the specimens aged at 232 °C was 35.9% and that for those at 66 °C was 28.1%. It is of interest to note that specimens that were not thermally aged (i.e., were maintained at room temperature, 23 °C) prior to immersion in deionized water for 72 weeks showed a decrease of 25.3%.

**Table 1.** Standard deviations of short beam shear strength for specimens immersed in deionized water after regimes of thermal aging.

Time of Immersion (Weeks)	Temperature of Thermal Aging for 8 h (°C)								
	23	66	93	121	149	177	204	232	260
0	1.41	2.25	1.12	1.50	1.51	1.62	0.60	2.66	2.46
4	3.08	0.90	3.48	1.25	1.59	2.84	1.20	2.23	1.85
8	2.29	1.67	1.16	0.63	1.17	2.22	2.52	1.79	5.23
12	2.35	2.51	1.40	1.74	1.20	1.50	2.29	3.28	5.61
16	1.59	1.74	0.47	3.03	0.41	1.54	2.56	2.67	2.31
24	1.97	2.22	0.62	2.92	2.74	2.32	3.19	1.58	5.96
36	2.50	1.81	1.81	2.06	1.08	1.90	1.77	1.41	5.86
48	2.22	1.44	2.38	2.27	1.83	2.94	0.64	5.15	3.48
72	2.45	1.89	2.97	2.67	2.24	3.21	1.21	5.41	5.98

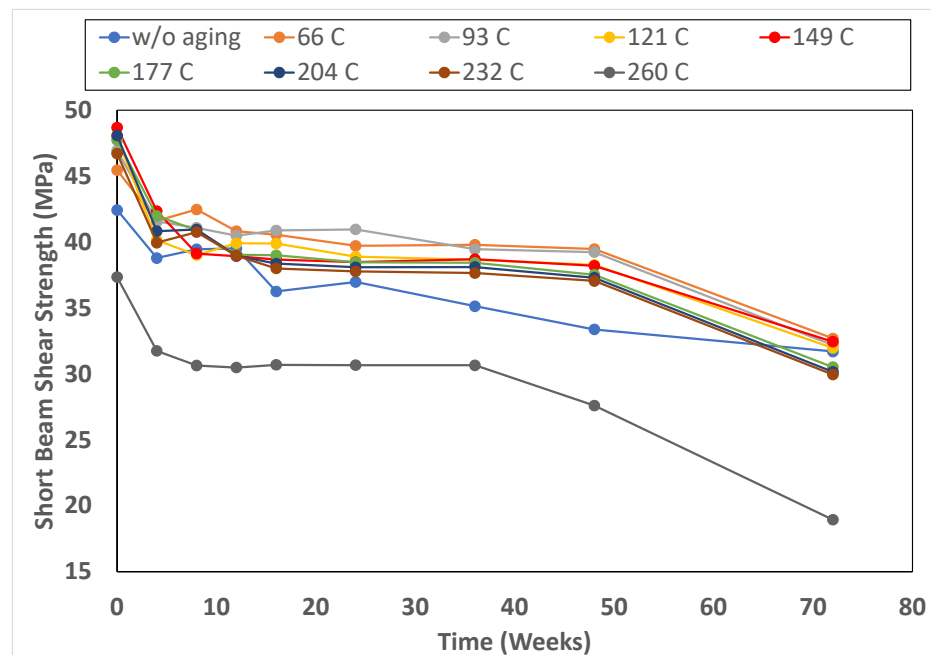


**Figure 9.** SBS strength as a function of time of immersion in deionized water and temperature of prior thermal aging for 8 h.

While the thermally aged specimens at all temperatures of aging showed a three-stage deterioration trend, the non-thermally aged specimens showed a gradual, but continuous, decrease with minor variation in levels from the beginning, as has been seen previously for SBS strength decrease due to hydrothermal exposure [87–89]. While fibers add to the strength and stiffness of the in-plane properties, the out-of-plane characteristics are often the limiting factor for laminate composites because they are dependent on the matrix. Resin characteristics, and hence those of the composite, such as toughness and interlaminar shear properties, are susceptible to rapid changes due to elevated temperatures, and even further on moisture uptake [90]. It is of interest to compare results of the sequential exposures considered in the current study with results of previous studies focused on hydrothermal exposure. Botelho et al. [91] reported decreases of about 28% in interlaminar shear strength of unidirectional carbon/epoxy prepreg-based composites after conditioning at 80 °C and 90% RH until moisture equilibrium was attained. Almudaihesh et al. [87] reported a reduction of 24.5% after immersion of prepreg-based, autoclave-cured carbon/epoxy in water at 90 °C for 43 days. In comparison, in the current study, a decrease of 12.5% in SBS strength was recorded after a similar period of immersion of 8 weeks after thermal aging for 8 h at 93 °C, indicating that the sequential exposure may have lower deteriorative effects than the simultaneous exposure to temperature and moisture (such as through elevated temperatures of immersion). It is noted that an equivalent level of reduction to the 24.5% reported [87] is only attained between 48 and 72 weeks of immersion in the current case, with 31.5% reduction being attained after the full period of 72 weeks of immersion.

Although the thermally aged specimens show significant overlap in performance, as seen in Figure 9, the specimen response can be divided into three groups, with the first being for thermal aging between 66 °C and 149 °C, the second being for those between 177 °C and 232 °C, and the third being specimens aged at 260 °C. Table 2 shows decreases from the initial level (i.e., after 8 h of thermal aging) to that determined after 72 weeks of immersion in deionized water, at the end of each of these stages, i.e., 4 weeks of immersion, 48 weeks of immersion, and 72 weeks of immersion. Taking into consideration the range of scatter in data, it can be seen that at the 48 and 72 h levels, deterioration generally increases with temperature of prior thermal aging. There is an initial increase at the 4-week level followed by a decrease and then an increase, mirroring effects of continued postcure.

It is also worthwhile to note that with the exception of specimens aged at 260 °C at the 48-week level, the effect of prior thermal aging results in a lower, or equivalent, level of deterioration than specimens immersed in water without aging, indicating that structures that have sufficient residual SBS strength after thermal aging could continue to perform similar to those just immersed in water. This is important from the perspective of assessing post-thermal event viability of continued use.

**Table 2.** Level of deterioration in SBS strength due to immersion in deionized water.

Period of Immersion (Weeks)	Temperature of Thermal Aging (°C)								
	Unaged	66	93	121	149	177	204	232	260
4	8.2	8.4	11.5	16.2	13.0	12.0	15.1	14.5	15.0
48	21.4	13.2	16.4	20.2	21.5	21.4	22.4	20.7	26.1
72	25.3	28.1	31.5	33.3	33.4	36.1	37.3	35.9	49.3

Given the previous discussion regarding competing effects of enhancing and deteriorative mechanisms resulting from thermal aging, it is important to note that previous studies on ambient cured wet layup composites have identified similar competing mechanisms resulting from immersion in water. Short periods of immersion have been noted to accelerate postcure mechanisms, resulting in an initial increase in mechanical characteristics with longer-term immersion, in turn resulting in decreases due to effects of plasticization and hydrolysis. In the current investigation, immersion was restricted to specimen specifically aged at temperature for 8 h only, and hence, the effect on the full range of levels cannot be clarified from this set. In contrast, the second case considered in this study of specimens thermally aged at 232 °C over the range of time periods up to 72 h prior to immersion in the aqueous solution, enables this effect to be further clarified. As seen in Figure 10, while the thermally unaged specimens show small levels of increase in SBS strength after immersion between 4 and 12 weeks followed by a decrease in line with earlier reported results for mechanical performance [16,31,92], the thermally aged specimens show a general decreasing trend with increases in the period of immersion except for specimens aged at 48 h and 72 h, where postcure effects are only seen between 4 and 8 weeks of immersion. For the range of 2–24 h of thermal aging, the drop in performance with time of immersion is gradual until the 48-week level, which is followed by a steep drop to about the same final level of SBS strength of between 29.95 MPa and 31.07 MPa, i.e., a decrease in that time period of 18.5 and 22.5%. A similar final level of strength and drop between the 48- and 72-week periods of immersion are seen, suggesting that the effects of immersion in water at longer periods of immersion are more dominant than the effect of temperature of prior thermal aging. This is an important finding when viewed in concert with the occurrence of the peak in SBS strength due to thermal aging at this temperature between 2 and 4 h as well as a fairly close level of the relaxation parameter,  $k$ , within this range, suggesting the existence of a threshold for drop in performance due to the second stage of immersion that may be independent of time of aging past a specific point represented by the initial point of maximum postcure. In light of this, it is illuminating to compare final levels of deterioration of SBS strength due to post-thermal aging immersion for 72 weeks as determined using both the initial non-thermally aged strengths and the level of maximum postcure determined as 50.13 MPa shown in Figure 8. When compared to this level, the percentage deterioration after 72 weeks of immersion in deionized water is the lowest after 1 h of previous thermal exposure at 34.8%, with all others being within a narrow band between 38.02–40.14 MPa with the levels increasing with the time of pre-immersion thermal aging.

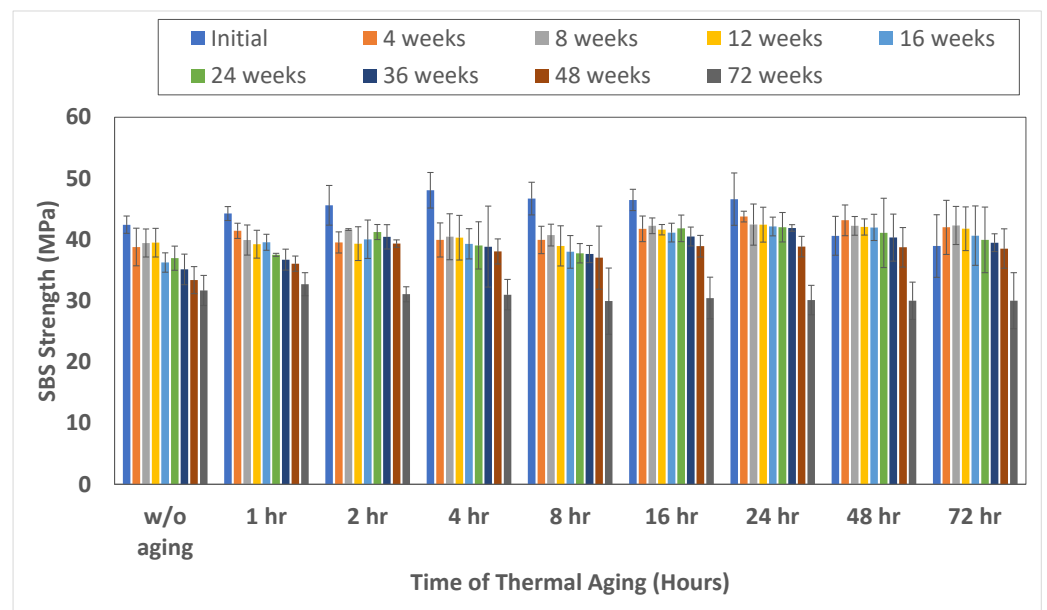


**Figure 10.** SBS strength as a function of time of immersion and period of prior thermal aging at 232 °C.

While this investigation considered only two specific cases of immersion after thermal aging it is beneficial, even to a limited extent, to understand the relative effects of the major factors under consideration: temperature of thermal aging, time of thermal aging, and time of immersion, following the averaging method used by Baghdad et al. [93]. For the purposes of this analysis, only results from exposure were considered, i.e., all results from unexposed specimens or unaged specimens were not included. Using their approach of averaging across the extremes and assessing the differences between the maximum and minimum values of residual performance, overall trends can be determined for conditions related to the two cases considered herein, i.e., (a) thermally aged for 8 h over a range of temperatures followed by immersion in deionized water for 72 h, and (b) thermally aged at 232 °C for a range of times followed by immersion in deionized water. In the first case, the overall change due to the period of immersion across all temperatures of thermal aging was −25.41%, whereas that of thermal aging temperature across all periods of immersion was −27.04%, indicating that for a specific period of thermal aging, the effects of temperature of thermal aging were only a bit greater than that of immersion time. In contrast in the second case, the overall change due to the period of immersion across all periods of thermal aging at 232 °C was −26.01%, whereas that of time of thermal aging across all periods of immersion was +3.8%, indicating the significantly greater effect of time of immersion. This further emphasizes the earlier discussed findings that effects of prior thermal aging at levels below 260 °C may not significantly hinder subsequent use/operation for fairly long periods of time under conditions of immersion as long as the residual SBS strength after thermal aging remained above the design threshold.

#### 4. Summary and Conclusions

The effect of sequential thermal aging followed by immersion in deionized water on the durability of carbon/epoxy composites was investigated in this paper. Effects are determined using SBS strength for characterization of mechanical characteristics and moisture kinetics through a two-stage diffusion model that incorporates a diffusion coefficient associated with the first stage of uptake and a time-dependent coefficient characteristic of the rate of polymer relaxation and damage due to water uptake representative of the second stage.

Thermal aging at all temperatures between 66 °C and 204 °C results in increases in SBS strength, indicating that postcure processes have a greater positive effect than that of

deterioration due to thermal aging. SBS strength is seen to decrease after 24 h of aging at 232 °C and after 8 h at 260 °C, at which point the highest value of SBS strength is also attained. When effects of full postcure are included, all specimens, however, show deterioration from the peak value over extended periods of thermal aging. Subsequent immersion in deionized water leads to a decrease in SBS strength for all specimens aged for 8 h, with the response being an initial decrease followed by an intermediate period between 12 and 48 weeks of immersion during which there is insignificant change in SBS strength, which is followed by a second period of rapid decrease. The maximum change is noted for specimens aged at 260 °C, with a decrease over the 72-week period of immersion being as high as 49% in comparison with a level of 28% for specimens at 66 °C and an average of 34.6% (with a standard deviation of 2.2%) for specimens between 93 °C and 232 °C, within which range the effects at the end of the 72-week period were similar.

For specimens aged at 232 °C and then immersed in water, the period of immersion is noted to have a substantially greater overall effect than the time of thermal aging, with the maximum decrease at the end of 72 weeks being 35.9%. A study of moisture kinetic characteristics shows that the diffusion coefficient increases with time of prior thermal aging for all temperatures up to 204 °C until the 16 h level, indicating effects of postcure which results in an increase in free volume as crosslink density increases. At 232 °C and above, the diffusion coefficient continues to increase, indicating deterioration in the bulk resin and the fiber-matrix interface and resulting in greater wicking along these microstructural defects in an auto-accelerative manner. The competition between the postcure and relaxation/deteriorative phenomena is also noted through the variation in the values of the relaxation coefficient. Trends in moisture uptake levels, both at the transition point and the maximum levels, are in accord with earlier results that link them to the degree of polymerization. Based on these tests, it is concluded that the effects of prior thermal aging at levels below 260 °C may not significantly hinder subsequent use/operation for fairly long periods of immersion time as long as the SBS strength after thermal aging prior to immersion remain above the design threshold values for continued use.

**Author Contributions:** V.M.K.: conceptualization, methodology, writing, analysis; S.H.: testing, data curation and checking, initial analysis. All authors have read and agreed to the published version of the manuscript.

**Funding:** This research received no external funding.

**Institutional Review Board Statement:** Not applicable.

**Informed Consent Statement:** Not applicable.

**Data Availability Statement:** The data presented in the study are available upon reasonable request from the corresponding author.

**Acknowledgments:** S.H. acknowledges the support of the Naval Academy.

**Conflicts of Interest:** The authors declare no conflict of interest.

## References

1. Helbling, C.; Abanilla, M.; Lee, L.; Karbhari, V.M. Issues of variability and durability under synergistic exposure conditions related to advanced polymer composites in the civil infrastructure. *Compos. Part A* **2006**, *37*, 1102–1110. [[CrossRef](#)]
2. Karbhari, V.M.; Abanilla, M. Design factors, reliability and durability prediction of wet layup carbon/epoxy used in external strengthening. *Compos. Part B* **2007**, *38*, 10–23. [[CrossRef](#)]
3. Spelter, A.; Bergmann, S.; Bielak, J.; Hegger, J. Long-term durability of carbon-reinforced concrete: An overview and experimental investigations. *Appl. Sci.* **2019**, *9*, 1651. [[CrossRef](#)]
4. Karbhari, V.M.; Hassanpour, B. Water, salt water, and concrete leachate solution effects on durability of ambient-temperature cure carbon-epoxy composites. *J. Appl. Polym. Sci.* **2022**, *139*, e52496. [[CrossRef](#)]
5. Scott, P.; Lees, J.M. Water, salt water, and alkaline solution uptake in epoxy thin films. *J. Appl. Polym. Sci.* **2013**, *130*, 1898–1908. [[CrossRef](#)]
6. Lettiere, M.; Frigione, M. Natural and artificial weathering effects on cold cured epoxy resins. *J. Appl. Polym. Sci.* **2001**, *119*, 1635–1645. [[CrossRef](#)]

7. Michel, M.; Ferrier, E. Effect of curing temperature conditions on glass transition temperature values of epoxy polymer used for wet layup applications. *Constr. Build. Mater.* **2020**, *231*, 117206. [[CrossRef](#)]
8. Feih, S.; Mouritz, A.P. Tensile properties of carbon fibers and carbon fibre-polymer composites in fire. *Compos. Part A* **2012**, *43*, 765–772. [[CrossRef](#)]
9. Li, C.; Xian, G. Experimental investigation of the microstructures and tensile properties of polyacrylonitrile-based carbon fibers exposed to elevated temperatures in air. *J. Eng. Fibers Fabr.* **2019**, *14*, 1558925019850010. [[CrossRef](#)]
10. Yin, Y.; Binner, J.G.P.; Cross, T.E.; Marshall, S.J. The oxidation behavior of carbon fibers. *J. Mater. Sci.* **1994**, *29*, 2250–2254. [[CrossRef](#)]
11. Feih, S.; Boiococchi, E.; Kandare, E.; Mathys, Z.; Gibson, A.G.; Mouritz, A.P. Strength degradation of glass and carbon fibers at high temperature. Proceedings of ICCM 17—17th International Conference on Composite Materials, Edinburgh, UK, 27 July–31 July 2009.
12. DePruneda, J.A.H.; Morgan, R.J. The effects of thermal exposure on the structural and mechanical integrity of carbon fibers. *J. Mater. Sci.* **1990**, *25*, 4776–4781. [[CrossRef](#)]
13. Brown, A.L. The decomposition behavior of thermoset carbon fiber epoxy composites in the fire environment. In Proceedings of the Combustion Institute Joint US Sections Meeting, Park City, UT, USA, 19–22 May 2013.
14. Adamson, M.J. Thermal-expansion and swelling of cured epoxy-resin used in graphite-epoxy composite-materials. *J. Mater. Sci.* **1980**, *15*, 1736–1745. [[CrossRef](#)]
15. Zhou, J.M.; Lucas, J.P. Hygrothermal effects of epoxy resin. Part I: The nature of water in epoxy. *Polymer* **1999**, *40*, 5505–5512. [[CrossRef](#)]
16. Nogueira, P.; Ramirez, C.; Torres, A.; Abad, M.J.; Cano, J.; Lopez, J.; Lopez-Bueno, I.; Barral, L. Effect of water sorption on the structure and mechanical properties of an epoxy resin system. *J. Appl. Polym. Sci.* **2001**, *80*, 71–80. [[CrossRef](#)]
17. Hahn, H.T. Residual-stresses in polymer matrix composite laminates. *J. Compos. Mater.* **1976**, *10*, 266–2678. [[CrossRef](#)]
18. Abanilla, M.A.; Li, Y.; Karbhari, V.M. Interlaminar and intralaminar durability characterization of wet layup carbon/epoxy used in external strengthening. *Compos. Part B* **2006**, *37*, 650–661. [[CrossRef](#)]
19. Mazor, A.; Broutman, L.J.; Eckstein, B.H. Effect of long-term water exposure on properties of carbon and graphite fiber reinforced epoxies. *Polym. Eng. Sci.* **1978**, *18*, 341–349. [[CrossRef](#)]
20. Ellis, T.S.; Karasz, F.E. Interaction of epoxy resins with water: The depression of glass transition temperature. *Polymer* **1984**, *25*, 664–669. [[CrossRef](#)]
21. Barton, J.M.; Greenfield, D.C.L. The use of dynamic mechanical methods to study the effect of absorbed water on temperature-dependent properties of an epoxy resin-carbon fibre composite. *Br. Polym. J.* **1986**, *18*, 51–56. [[CrossRef](#)]
22. Tomblin, J.S.; Salah, L.; Ng, Y.C. *Determination of Temperature/Moisture Sensitive Composite Properties*; DOT/FAA/AR-0 1/40; US Department of Transportation, Federal Aviation Administration: Washington, DC, USA, 2001.
23. Rajaraman, A.N.; Boay, C.G.; Srikanth, N. Effect of curing on the hygrothermal behavior of epoxy and its carbon composite materials. *Compos. Commun.* **2020**, *22*, 100507. [[CrossRef](#)]
24. Ghorbel, I.; Valentin, D. Hydrothermal effects on the physico-chemical properties of pure and glass fiber reinforced polyester and vinylester resins. *Polym. Compos.* **1993**, *14*, 324–334. [[CrossRef](#)]
25. Marshall, J.M.; Marshall, G.P.; Pinzelli, R.F. The diffusion of liquids into resins and composites. *Polym. Compos.* **1982**, *3*, 131–137. [[CrossRef](#)]
26. Schultheisz, C.R.; Schutte, C.L.; McDonough, W.G.; Macturk, K.S.; McAuliff, M.; Kondagunta, S.; Hunston, D.L. *Effect Temperature and Fiber Coating on the Strength of E-Glass Fibers and the E-Glass/Epoxy Interface for Single Fiber Fragmentation Samples Immersed in Water*; ASTM STP 1290; ASTM: Conshohocken, PA, USA, 1986; pp. 103–131.
27. Karbhari, V.M. Long term hydrothermal aging of carbon-epoxy materials for rehabilitation of civil infrastructure. *Compos. Part A* **2022**, *153*, 106705. [[CrossRef](#)]
28. Karbhari, V.M.; Chin, J.W.; Hunston, D.; Benmokrane, B.; Juska, T.; Morgan, R.; Lesko, J.J.; Sorathia, V.; Reynaud, D. Durability Gap Analysis for FRP Composites in Civil Infrastructure. *ASCE J. Compos. Constr.* **2003**, *7*, 238–247. [[CrossRef](#)]
29. Holloway, L.C. A review of the present and future utilization of FRP composites in the civil infrastructure with reference to their important in-service properties. *Constr. Build. Mater.* **2010**, *24*, 2419–2445. [[CrossRef](#)]
30. Uthaman, A.; Xian, G.; Thomas, S.; Wang, Y.; Zheng, Q.; Liu, X. Durability of an epoxy resin and its carbon fiber-reinforced polymer composite upon immersion in water, acidic, and alkaline solutions. *Polymers* **2020**, *12*, 614. [[CrossRef](#)]
31. Marouni, S.; Curtil, L.; Hamelin, P. Composites realized by hand lay-up process in a civil engineering environment: Initial properties and durability. *Mater. Struct.* **2008**, *41*, 831–851. [[CrossRef](#)]
32. Tual, N.; Carrere, N.; Davies, P.; Bonnemains, T.; Lolive, E. Characterization of seawater aging effects on mechanical properties of carbon/epoxy composites for tidal turbine blades. *Compos. Part A* **2015**, *78*, 380–389. [[CrossRef](#)]
33. Kootsookos, A.; Mouritz, A.P. Seawater durability of glass- and carbon-polymer composites. *Compos. Sci. Technol.* **2004**, *64*, 1503–1511. [[CrossRef](#)]
34. Rubino, F.; Nistico, A.; Tucci, F.; Carlone, P. Marine application of fiber reinforced composites: A review. *J. Mar. Sci. Eng.* **2020**, *8*, 26. [[CrossRef](#)]
35. Davies, P.; Rajapakse, Y.D.S. (Eds.) *Durability of Composites in a Marine Environment*; Springer: Dordrecht, The Netherlands, 2014.

36. Colin, X.; Verdu, J. Strategy for studying thermal oxidation of organic matrix composites. *Compos. Sci. Technol.* **2005**, *65*, 411–419. [[CrossRef](#)]
37. Bowles, K.J.; Jayne, D.; Leonhardt, T.A.; Bors, D.J. Thermal Stability Relationships between PMR-15 Resin and Its Composites. NASA TM 106285. 1993. Available online: <https://ntrs.nasa.gov/citations/19940017015> (accessed on 5 September 2022).
38. Meador, M.A.B.; Lowell, C.E.; Cavano, P.J.; Herrera-Fierro, P. On the oxidative degradation of nadic capped polyimides I: Effect of thermocycling on weight loss and crack formation. *High Perform. Polym.* **1996**, *8*, 363–379. [[CrossRef](#)]
39. Tandon, G.P.; Pochiraju, K.V.; Schoeppner, G.A. Modeling of oxidative development in PMR-15 resin. *Polym. Degrad. Stab.* **2006**, *91*, 1861–1869. [[CrossRef](#)]
40. Reifsnider, K.L.; Case, S. Mechanics of temperature driven long term environmental degradation of polymer-based composite systems. In Proceedings of the ASME Symposium on Durability and Damage Tolerance, San Francisco, CA, USA, 12–17 November 1995.
41. Zhuang, H.; Wightman, J.P. The influence of surface properties on carbon fiber/epoxy matrix interfacial adhesion. *J. Adhes.* **1996**, *62*, 213–245. [[CrossRef](#)]
42. Wimolkiasak, A.S.; Bell, J.P. Interfacial shear strength and failure modes of interface modified graphite-epoxy composites. *Polym. Compos.* **1989**, *10*, 162–172. [[CrossRef](#)]
43. Gardiner, C.P.; Mathys, Z.; Mouritz, A.P. Tensile and compressive properties of FRP Composites with localized fire damage. *Appl. Compos. Mater.* **2002**, *9*, 353–367. [[CrossRef](#)]
44. Mouritz, A.P.; Gibson, A.G. *Fire Properties of Polymer Composite Materials*; Springer: Dordrecht, The Netherlands, 2006.
45. Mouritz, A.P.; Feih, S.; Kandare, E.; Mathys, Z.; Gibson, A.G.; DesJardin, P.E.; Case, S.W.; Lattimer, B.Y. Review of fire structured modeling of polymer composites. *Compos. Part A* **2009**, *40*, 1800–1814. [[CrossRef](#)]
46. Tran, P.; Nguyen, Q.T.; Lau, K.T. Fire performance of polymer-based composites for maritime infrastructure. *Compos. Part B* **2018**, *155*, 31–48. [[CrossRef](#)]
47. Firmo, J.P.; Correia, J.R.; Bisby, L.A. Fire behavior of FRP-strengthened reinforced concrete structural elements: A state-of-the-art review. *Compos. Part B* **2015**, *80*, 198–216. [[CrossRef](#)]
48. Singh, S.B.; Sethi, A. A review of performance of fiber reinforced polymer strengthened structures under fire exposure. *Proc. Indian Natl. Sci. Acad. USA* **2017**, *83*, 521–532.
49. Bazli, M.; Abolfazli, M. Mechanical properties of fibre reinforced polymers under elevated temperatures: An overview. *Polymers* **2020**, *12*, 2600. [[CrossRef](#)]
50. Karbhari, V.M.; Xian, G.; Hong, S.K. Effect of thermal exposure on carbon fiber reinforced composites used in civil infrastructure rehabilitation. *Compos. Part A* **2021**, *149*, 106570. [[CrossRef](#)]
51. Maravenas, C.; Miamis, K.; Vrakas, A.A. Fiber-reinforced polymer strengthened/reinforced concrete structures exposed to fire: A review. *Struct. Eng. Int.* **2012**, *22*, 500–513. [[CrossRef](#)]
52. Roberts, A.F. Thermal radiation hazards from releases of LPG from pressurized storage. *Fire Saf. J.* **1981**, *4*, 197–212. [[CrossRef](#)]
53. Hoffman, E.; Skidmore, T.E. Radiation effects on epoxy/carbon fiber composite. *J. Nucl. Mater.* **2009**, *392*, 371–378. [[CrossRef](#)]
54. Holliday, R.J.; Gibson, A.G.; Humphrey, J.; DiModica, P.; Christko, S.; Kotsikas, G. Post-fire structural integrity of composite gratings for offshore platforms. In Proceedings of the SPE Offshore Europe Oil and Gas Conference, Aberdeen, UK, 3–6 September 2013. Paper # SPE-166587-M6.
55. Fire Fighting with Passive Resistance. *The Engineer*, 18 October 1990.
56. Brkic, D.; Praks, P. Probability analysis and prevention of offshore oil and gas accidents: Fire as a cause and a consequence. *Fire* **2021**, *4*, 71. [[CrossRef](#)]
57. Vielvoye, R. Piper Alpha Report to Spawn Many Changes in UK Regulations. *Oil Gas J.* **1990**, *88*, 21–24.
58. Dewhurst, D.W. The Influence of Fire on the Design of Polymer Composite Pipes and Panels for Offshore Structures. Ph.D. Thesis, University of Salford, Salford, UK, 1997.
59. Xiang, Z.D.; Jones, F.R. Thermal-spike-enhanced moisture absorption by polymer-matrix carbon-fibre composites. *Compos. Sci. Technol.* **1997**, *57*, 451–461. [[CrossRef](#)]
60. Hough, J.A.; Karad, S.K.; Jones, F.R. The effect of thermal spiking on moisture absorption, mechanical and viscoelastic properties of carbon fibre reinforced epoxy laminates. *Compos. Sci. Technol.* **2005**, *65*, 1299–1305. [[CrossRef](#)]
61. Adamson, N.J. *A Model of the Thermal Spike Mechanism in Graphite Epoxy Laminates*; NASA TM-8429 Nine; NASA: Washington, DC, USA, 1982.
62. Loos, A.C.; Springer, G.S. Effects of thermal spiking on graphite-epoxy composites. *J. Compos. Mater.* **1979**, *13*, 17–34. [[CrossRef](#)]
63. Lu, Z.; Xian, G.; Li, H. Effects of thermal aging on the water uptake behavior of pultruded BFRP plates. *Polym. Degrad. Stab.* **2014**, *110*, 216–224. [[CrossRef](#)]
64. Hamedi, Y.K.; Levent, A.; Altan, M.C. Thermal history effects on moisture absorption of fiber-reinforced polymer composites. In *AIP Conference Proceedings*; AIP Publishing LLC.: Melville, NY, USA, 2017; Volume 1914, p. 030012. 5p.
65. Thomas, J.L. The interface region in glass fibre-reinforced epoxy resin composites II: Water absorption, voids, and the interface. *Composites* **1995**, *26*, 477–485. [[CrossRef](#)]
66. Karbhari, V.M. E-Glass/Vinylester composites in aqueous environments: Effects on short-beam shear strength. *ASCE J. Compos. Constr.* **2004**, *8*, 148–156. [[CrossRef](#)]

67. ASTM D2344/D2344 M-16; Standard Test Method for Short-Beam Strength of Polymer Matrix Composite Materials and Their Laminates. ASTM International: West Conshohocken, PA, USA, 2016.
68. MIL-HDBK-17/1 *Composite Materials Handbook Volume One: Polymer Matrix Components Guidelines for Characterization of Structural Materials*; Department of Defense: Washington, DC, USA, 1997.
69. ASTM D3418-21; Standard Test Method for Transition Temperatures and Enthalpies of Fusion and Crystallization of Polymers by Differential Scanning Calorimetry. ASTM International: West Conshohocken, PA, USA, 2021.
70. Browning, C.E. The mechanisms of elevated temperature property losses in high performance structural epoxy resin materials after exposure to high humidity environments. *Polym. Eng. Sci.* **1978**, *18*, 16–24. [[CrossRef](#)]
71. Shen, C.H.; Springer, G.S. Moisture adsorption and desorption of composite materials. *J. Compos. Mater.* **1976**, *10*, 2–20.
72. Bagley, E.; Long, F.A. Two-stage sorption and desorption of organic vapors in cellulose acetate. *J. Am. Chem. Soc.* **1955**, *77*, 2172–2182. [[CrossRef](#)]
73. Bao, L.-R.; Yee, A.F.; Lee, C.Y.-C. Moisture absorption and hydrothermal aging in a bisaleimide resin. *Polymer* **2001**, *42*, 7327–7333. [[CrossRef](#)]
74. Jackson, M.; Kaushik, M.; Nazarenko, S.; Ward, S.; Maskell, R.; Wiggins, J. Effect of free volume hole-size on fluid ingress of glass epoxy networks. *Polymer* **2011**, *52*, 4528–4535. [[CrossRef](#)]
75. Toscano, A.; Pitarresi, G.; Scafidi, M.; Di Filippo, M.; Spadaro, G.; Alessi, S. Water diffusion and swelling stresses in highly cross-linked epoxy matrices. *Polym. Degrad. Stab.* **2016**, *133*, 255–263. [[CrossRef](#)]
76. Xian, G.; Karbhari, V.M. DMTA based investigation of hygrothermal ageing of an epoxy system used in rehabilitation. *J. Appl. Polym. Sci.* **2007**, *104*, 1084–1094. [[CrossRef](#)]
77. Marom, G. Environmental effects on fracture mechanical properties of polymer composites. In *Application of Fracture Mechanics to Composite Materials*; Frederich, K., Ed.; Chapter 5; Elsevier: New York, NY, USA, 1989.
78. Woo, M.; Piggott, M.R. Water absorption of resins and composites IV. *Water transport in fiber reinforced plastics*. *J. Compos. Technol. Res.* **1988**, *10*, 20–24.
79. Berens, A.R.; Hopfenberg, H.B. Diffusion and relaxation in glassy polymer powders: 2. Separation of diffusion and relaxation parameters. *Polymer* **1978**, *19*, 489–496. [[CrossRef](#)]
80. Tang, J.; Springer, G.S. Effects of cure and moisture on the properties of Fiberite 976 resin. *J. Compos. Mater.* **1988**, *22*, 2–14. [[CrossRef](#)]
81. Chatterjee, A.; Gillespie, J.W., Jr. Moisture absorption behavior of epoxies and their S2 glass composites. *J. Appl. Polym. Sci.* **2008**, *108*, 3942–3951. [[CrossRef](#)]
82. de Parscau du Plessix, B.; Jacquemin, F.; Lefebure, P.; Le Corre, S. Characterization and modeling of the polymerization-dependent moisture absorption behavior of an epoxy-carbon fiber-reinforced composite material. *J. Compos. Mater.* **2016**, *50*, 2495–2505. [[CrossRef](#)]
83. Zavatta, N.; Rondina, F.; Falaschatti, M.P.; Donati, L. Effect of thermal aging on the mechanical strength of carbon fibre reinforced epoxy composites. *Polymers* **2021**, *13*, 2006. [[CrossRef](#)]
84. Vora, K.; Yo, T.; Islam, M.; Habibi, M.; Minaie, B. Evolution of mechanical properties during cure for out-of-autoclave carbon-epoxy prepregs. *J. Appl. Polym. Sci.* **2015**, *132*, 41548.
85. Akay, M.; Spratt, G.R.; Meenan, B. The effects of long-term exposure to higher temperatures on the ILSS and impact performance of carbon fibre reinforced bismaleimide. *Compos. Sci. Technol.* **2003**, *63*, 1053–1059. [[CrossRef](#)]
86. Findley, W.N. Mechanisms and mechanics of creep of plastics. *SPE J.* **1960**, *16*, 57–65.
87. Almudaihesh, F.; Grigg, S.; Holford, K.; Pullin, R.; Eaton, M. An assessment of the effect of progressive water absorption on the interlaminar strength of unidirectional carbon/epoxy composites using acoustic emission. *Sensors* **2021**, *24*, 4351. [[CrossRef](#)]
88. Meng, M.; Rizvi, M.J.; Grove, S.M.; Le, H.R. Effects of hygrothermal stress on the failure of CFRP composites. *Compos. Struct.* **2015**, *133*, 1024–1035. [[CrossRef](#)]
89. Joshi, O.K. The effect of moisture on the shear properties of carbon fibre composites. *Composites* **1983**, *14*, 196–200. [[CrossRef](#)]
90. Alam, P.; Robert, C.; Bradaigh, C.M. Tidal turbine blade composite—A review on the effects of hygrothermal aging on the properties of CFRP. *Compos. Part B* **2018**, *149*, 248–259. [[CrossRef](#)]
91. Botelho, E.C.; Pardini, L.C.; Rezende, M.C. Hygrothermal effects on the shear properties of carbon fiber/epoxy composites. *J. Mater. Sci.* **2006**, *41*, 7111–7118. [[CrossRef](#)]
92. Abanilla, M.A.; Li, Y.; Karbhari, V.M. Durability characterization of wet layup graphite/epoxy composites used in external strengthening. *Compos. Part B* **2005**, *37*, 200–212. [[CrossRef](#)]
93. Baghdad, A.; El Mabrouk, K.; Vaudreuil, S.; Nouneh, K. Effects of high operating temperatures and holding times on thermo-mechanical and mechanical properties of autoclaved epoxy/carbon composite laminates. *Polym. Compos.* **2022**, *43*, 862–873. [[CrossRef](#)]